Minimizing Environmental Impact of Cruise Flights using Meta-heuristic and Optimal Control Optimizations

I.Govers

Under supervision of Dr. J. Sun and Prof. Dr. Ir. J.M. Hoekstra

Control & Operations, Faculty of Aerospace Engineering
Delft University of Technology, Delft, The Netherlands

***Abstract*—Aviation has a negative impact on the environment. As the number of flights is expected to increase, the total environmental impact of aviation will continue to worsen. New solutions are required to mitigate these effects. Aircraft Trajectory Optimization For Environmental Impact (TOFEI) can help reduce the impact of aircraft pollutants while also facilitating an increase in the number of flights. Whereas previous studies have shown that TOFEI can be effective in mitigating the footprint of aviation, their scope is limited. An applicable model should include wind, variable Mach number and an appropriate environmental impact metric. This paper presents the Trajectory Optimizer for Environmental Purposes (TOEP), which bridges the existing gap. The approach comprises two models, a genetic algorithm and a direct collocation model. The former finds climate-optimal trajectories using a meta-heuristic search technique, while the latter solves the problem using optimal control in CasADi. As direct collocation provides faster and more accurate results, the genetic algorithm is used to verify the direct collocation model. The algorithm uses the open aircraft performance model OpenAP. Results show that the environmental impact of flights could be reduced by as much as 6.6% when fully optimizing for this metric. The impact differs significantly between short haul flights and long haul flights, with 1.2% environmental cost reduction for the former and 2.7% for the latter. Pareto fronts are utilized to investigate the relationship between operating cost and the environmental cost.**

Nomenclature

Acronyms

CI	Cost Index
DC	Direct Collocation
EC	Environmental Cost
GA	Genetic Algorithm
SOC	Simple Operating Cost
TOEP	Trajectory Optimization for Environmental Purposes
TOFEI	Trajectory Optimization For Environmental Impact

Symbols

$\boldsymbol{w}$	Wind vector
V_{tas}	True airspeed
u(t)	Control variable vector
x(t)	State variable vector
y(t)	Discretized variable vector

I. Introduction

The aviation industry is one of the major contributors to anthropogenic climate change and air quality deterioration. Governments and institutions have started to create awareness amongst civilians, and incentivise alternatives to flying. However, flying is expected to remain popular for the coming years with an average growth of 3.7% annually [1]. As a result, the International Civil Aviation Organization predicts that the amount of CO_2 produced by the industry will more than double within twenty years [2].

CO_2, NO_x, H_2O, CO, SO_x and Hydrocarbons (HC) are all part of the engine exhaust and can also have serious impact by either contributing to the creation of greenhouse gasses or by being a greenhouse gas itself. The impact of aircraft emissions on human health through air quality deterioration is also non-trivial: the approximate amount of premature deaths because of air quality deterioration due to aircraft pollution is 16,000 [3].

To compare the impact different species have, certain climate metrics have been developed. Radiative forcing establishes the impact of a species on the balance of incoming and outgoing energy (W/m^2) in the earth system [4]. The global temperature potential goes one step further in the cause-effect chain. It is a measure of the increase in surface temperature due to a pulse emission, relative to that of CO_2. It integrates the effect of the radiative forcing to obtain the temperature change on a scale of 10, 20, 50 or 100 years [5]. Some scientists have taken the leap to evaluate the monetary cost of emission pollutants. Whereas the cost of environmental impact does add additional uncertainty to the problem, the metric is simple to convey to decision makers who do not have a background in environmental impact studies. These metrics thus represent an extension from a technical perspective to a human impact perspective.

To mitigate the negative effects of aircraft pollution, three general strategies are aircraft design, fleet planning and aircraft operational planning. The development of novel aircraft which have a radically different design can significantly reduce emissions through aerodynamic

gains and different propulsive concepts [6]. Secondly, airlines can contribute by fleet planning, where they phase out more polluting aircraft and purchase cleaner ones. Research into fleet renewal programs indicates that the global airline fleet becomes 2% more environmentally friendly on a yearly basis [7]. Finally, aircraft operations can be optimized to reduce the climate impact of aviation. An investigation by Eurocontrol in 2020 [8] found that inefficiencies in European air traffic management network results in an additional 9 to 11% fuel burned.

This project focuses on optimizing aircraft operations, specifically considering Trajectory Optimization For Climate Impact (TOFEI). The essence of such optimization is to find trajectories which minimize a particular climate cost function. Different configurations of green objective functions are available, ranging from minimizing the fuel used to minimizing the global warming caused by a flight [9, 10].

In the past, considerable research has been performed on TOFEI. Because there is no consensus on how environmental impact can be assessed best, researchers have come up with a wide range of different approaches to optimize aircraft trajectories for green purposes. They can generally be divided into single objective optimization and multiple-objective optimization. Whereas the former has one global optimum, the latter yields Pareto optimality, in which a trade-off can be made between the multiple objective function values. In Figure 1, an arbitrary Pareto front is given for the objectives f1 and f2. By decreasing the cost of f2, the optimal cost of f1 is inherently increased. Such a front can only be obtained when a conflicting objective is in place. To the right of the Pareto front are the points which are not optimal but feasible, while the infeasible cost combinations lie to the left of the Pareto front. An example is the study performed by Pervier et al. (2011) [11]. The researchers developed a model which is able to optimize for both CO_2 emission and time optimality. The study finds that the most extreme solution for time-optimality produces up to 10% more CO_2 than a fuel-optimal trajectory.

Visser and Hartjens (2020) [12] perform multi-objective optimization on a number of different parameters. Using pre-defined weights, the noise, CO_2, time and NO_x are combined into a cost function. The study simplifies the problem to 2D, assuming the horizontal profile is known a priori. Whereas this does reduce computational effort, it will yield local optima as the optimal horizontal trajectory is assumed or optimized separately.

One of the leading papers in the field of TOFEI with a single objective is the work presented by Yamashita et al. (2020) [10]. The researchers developed *Airtraf*, a model finding trajectories that minimize temperature change due to the aircraft emissions. In order to accurately determine what this temperature response is, the chemistry-climate model *EMAC* [13] is used. The researchers find that in specific conditions the temperature increase can be limited to 67% compared to a cost-optimal solution for trans-

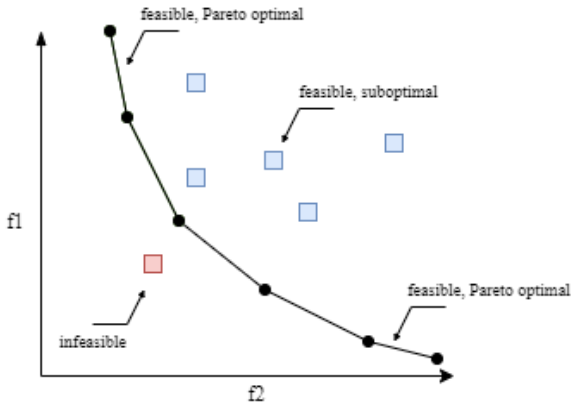

Figure 1: *Basic example of a Pareto front. Points lying on the black line represent optimal combinations of objective f1 and f2. Points to the left of the front are infeasible, while points to the right of the line are suboptimal.*

Atlantic flights. Similar objective functions can be observed in other studies [14, 15, 16], where more modest climate models are utilized.

Tian et al. [17, 18] take the leap to define the Green Direct Operating Cost, which combines the direct operating cost of a trajectory with the monetary cost associated with aircraft pollutants. The advantage of such a metric is that it simplifies the impact for policymakers who might not have a background in environmental sciences. The researchers use the market value of the European emission trading scheme to come up with a specific cost per unit weight emitted for each species. The results of the study show that of all cost made on a conventional flight, 50% of it is due to environmental cost.

Although significant research has been performed and results indicate that TOFEI can help contribute in mitigating aviation's environmental impact, there is a gap to bridge before the models are sufficiently realistic for implementation. The limitations comprise unreasonable assumptions, such as no wind or a constant Mach number throughout the flight. Whereas these problems have been tackled individually in different studies, there has not been a single study with a comprehensive scope. Moreover, optimization models will mainly see usage by stakeholders such as airlines, air traffic control and policymakers. These parties currently have no access to the developed models, as the tools have not been created for open access.

The aim of this paper is to present an open approach which takes the next step in TOFEI research by incorporating a more realistic scope compared to the status quo: considering wind, variable Mach number and a comprehensive environmental impact metric. This serves the two ultimate goals of this project: to foster research towards TOFEI and to increase awareness about its effects.

To this end, the Trajectory optimizer for Environmental Purposes (TOEP) is created. The approach consists of two environmental optimization models. The first uses evolutionary search to converge to the optimum, specific-

ally with genetic algorithms. This model is used to verify the results from the second model. The second model is based on transcription of the optimal control problem using direct collocation and is solved using non-linear programming. Both models use wind data obtained from the ERA5 hourly re-analysis model [19]. The optimizer is completely open access, and is based on the Open Aircraft Performance model [20]. The tool allows for varying Mach number and optimizes the horizontal and vertical path simultaneously. To demonstrate the impact of the approach, a case study is performed for a set of city pairs. Besides, the impact of the objective is assessed using a Pareto front. Currently, the approach is solely concerned with the cruise phase of the trajectory. This is the most important phase to consider, as aircraft spend most of their time in the air being in this phase while it is also the less constrained compared to landing and take-off [21].

This paper is organized as follows. In section II, the framework in which the optimization models will be constructed is presented. section III describes the set-up and fundamentals of the two numerical models are described. section IV presents the benchmark studies. They are performed to verify the approach using simple (known) solutions. In section V, a comparison between the environmental impact of actual and optimal trajectories is given. Besides, this section provides insights in the trade-off between environmental cost and operating cost as an objective. Finally, section VI concludes the study.

II. Problem Formulation

A. Aircraft Performance modelling

The equations of motion of a conventional fixed-wing aircraft can be reduced from a six-degree of freedom model to a three-degree of freedom point-mass model. The underlying assumption here is that all forces act through the centre of gravity, removing any moments. Besides, the large temporal scale of the problem implies the flight path angle and heading angle can change instantaneously, meaning that they do not require a dynamic description. Finally, the flight path angle is assumed to align with the pitch angle and the heading angle coincides with the yaw angle. This leads to the set of equations presented in Equations 1-5.

$$\frac{dx}{dt} = V_{tas} \cdot cos(\gamma) \cdot cos(\psi) + w_x \tag{1}$$

$$\frac{dy}{dt} = V_{tas} \cdot cos(\gamma) \cdot sin(\psi) + w_y \tag{2}$$

$$\frac{dh}{dt} = V_{tas} \cdot cos(\gamma) \tag{3}$$

$$\frac{dV_{tas}}{dt} = \frac{T - D(m, V_{tas}, h, \gamma)}{m} - g_0 \cdot sin(\gamma) \tag{4}$$

$$\frac{dm}{dt} = -FF(m, V_{tas}, h) \tag{5}$$

The first three equations describe the kinematic behaviour of the aircraft. Here, the relation of the positional coordinates *x, y, h* with respect to the true airspeed V_{tas}, heading angle ψ, flight path angle γ and directional wind *w* are given. Equation 4 is known as the dynamic equation, describing the change in true airspeed given the thrust *T*, Drag *D* and flight path angle γ. The fuel consumption equation (5) completes the model. g_0 is the earth gravitational constant at ground level in m/s^2.

The underlying aircraft performance model is OpenAP, which is built upon aircraft surveillance data and open literature models. It includes the most important aircraft data and kinematic libraries required to model aircraft performance, for the 27 most common aircraft. An important aspect of OpenAP for this study is the emission module, which is able to calculate the amount of pollutant per species. When compared to similar toolkits such as BADA [22], OpenAP finds very similar characteristics. A clear advantage of OpenAP over BADA is the fact that it is an open-source toolkit, which is why this is the selected aircraft performance model.

B. Environmental & Weather modelling

A monetary metric is used to model the environmental impact of a flight, as it is simple to convey while it also creates flexibility for the optimization problem because of its high-level approach. The metric is based on a recent study by Grobler et al. (2019) [23]. They estimate the climate and air quality cost based on a reduced-order climate model. The researchers consider both CO_2 and non-CO_2 emissions, of which the radiative forcing values are estimated for different phases of flight. These are used to obtain the global temperature change due to the emissions. By considering the health, welfare and ecological cost of these temperature changes, the monetary cost of emitting certain species is obtained. Naturally, there are some uncertainties introduced when converting between radiative forcing and monetary cost, which results in a range of cost values for each species. In Table I, the mean unit emission cost values are presented for each species. Between brackets, the 5^{th} and 95^{th} percentile are presented. Unless stated otherwise, the mean cost values are used throughout this study. For an overview of the specific distribution for each species, please refer to appendix subsection B.

The wind data used for this research is taken from the ERA5 model, provided by the European Centre for

Species	Climate (USD/tonne)	Air Quality (USD/tonne)
CO_2	45 (6.7, 120)	N/A
NO_x	-940 (-2600, -120)	21 000 (3300, 69 000)
SO_x	-20 000 (-53 000, -2700)	30 000 (4700, 100 000)
H_2O	2.8 (0.41, 7.5)	N/A
HC	N/A	2300 (360, 7300)
CO	N/A	7000 (980, 25 000)

Table I: *Global aggregate cost of emissions in cruise phase as found by Grobler et al. (2019) [23] for a 3% discount rate. Between brackets, the 5th and 95th percentile are provided.*

Medium-Range Weather Forecasts. The model provides historical hourly estimates of wind speed, using data assimilation [19]. Using multi-variable ridge regression, a five-degree multi-variable polynomial is fitted on the wind data points between the origin and destination. The ridge regression allows for a regularization of the error, preventing over-fitting [24]. More information about the construction of the wind polynomial is available in the appendix.

C. Optimization Criteria

There are two areas of interest when considering the optimization criteria. First, the constraints define the bounds within which the optimizer can search for the optimum solution. In Table II, the main constraints imposed on the optimization problem are presented. The departure and destination airport are given to the model by the user, and are converted to x, y coordinates using the OpenAP toolkit. The lower altitude limit is 9,000 meters, which is below the standard cruising altitude regime of 10,000 - 13,000 meters to allow the optimum to be found without enlarging the search space to unreasonable quantities. The variables which are taken from aircraft data in OpenAP are in bold. The user does not have to change these values on a regular basis. The initial mass is set to 80% of the maximum take-off weight, which is an arbitrary value chosen because it allows for long flights while keeping the simulation semi-realistic. Finally, the flight path angle is kept zero at all times, meaning that the model will search for a constant optimal cruise altitude.

The main cost function used throughout this study is Environmental Cost (EC). The monetary cost of the emission of different pollutants is implemented according to Equation 6. In this equation, P is the total number of species included in the optimization, while α is the unit emission cost for each respective species in USD per kg, as found in Table I. m_i represents the mass of the emitted pollutants, which is dependent on the mass flow, true airspeed and altitude.

$$\text{EC} = \sum_{i=0}^{P} \alpha_i \cdot m_i(ff, V_{tas}, h) \tag{6}$$

To adequately assess the effects of TOEP, it is important to consider the operating cost. Therefore, a Cost Index is used to model the actual operating cost. This ratio of time cost and fuel cost (CI = time cost weight / fuel cost weight) is frequently used in cost functions associated with aviation.

The Simple Operating Cost (SOC) is specified in Equation 7, and is based on the implementation by Yamashita et al. (2020) [10]. Here, c_t is the cost per second flown, which includes the flight crew, cabin crew and aircraft maintenance. c_f is the unit cost of fuel, respectively. m_f represents the total fuel usage, while t_f represents the total flown time. The cost index value is different for every airline. For this study, c_t and c_f are taken to be 0.75 (USD)s^{-1} and 0.51 (USD)kg^{-1}, respectively [25]. If not mentioned specifically, the cost index is assumed to be 0.5.

$$\text{SOC} = \text{CI} \cdot c_t \cdot t_f + (1 - \text{CI}) \cdot c_f \cdot m_f \tag{7}$$

To allow for a quantitative analysis of the effects of environmental optimization on the SOC, a mixed objective function is established in Equation 8. In this equation, l_{soc} and l_{ec} are the weights given to the SOC and EC respectively. Their sum is always equal to 1.

$$\text{Mix} = l_{soc} \cdot \text{SOC} + l_{ec} \cdot \text{EC} \tag{8}$$

III. Numerical Models

Two methods are deployed to extract optimal trajectories. One of the two models uses the gradient-based search method called Direct Collocation (DC), which treats the problem as an optimal control problem. The second model is a Genetic Algorithm (GA), which employs a heuristic search to find the global optimal solution. The latter model is used to verify the former, as the DC model will generally be able to find more accurate solutions. This section will describe some inner working and setup of both of these models.

A. Direct Collocation

Direct collocation is a method to transcribe an optimal control problem to a non-linear programming problem. Here, one aims to find the control input that minimizes a given objective function. The generic notation for this type of problem is specified in Equation 9 [26]. Here, *J* represents the cost function value. *E* is the Mayer term, which represents the cost of starting (at $t = t_0$) and ending (at $t = t_F$). *L* is the Lagrange term, which describes the cost built up along the trajectory. Both *E* and *L* are assumed to be twice differentiable. The first constraint is known as the dynamic constraint, ensuring that the real system dynamics match the derivative of the estimated states. The path constraints $\boldsymbol{h}(\cdot)$ describe bounds on the variables along the trajectory, while the boundary constraints $\boldsymbol{g}(\cdot)$ set the limits for all control and state variables.

$$\underset{t,\mathbf{x},\mathbf{u}}{\text{Min}}\ J = E(t_0, t_F, \mathbf{x}(t_0), \mathbf{x}(t_F)) + \int_{t_0}^{t_F} L(t, \mathbf{x}(t), \mathbf{u}(t))dt \tag{9}$$

Subject to:

$$\dot{\boldsymbol{x}}(t) = \mathbf{f}(t, \mathbf{x}(t), \mathbf{u}(t)) \qquad t \in [t_0, t_f]$$

$$\boldsymbol{h}(t, \boldsymbol{x}(t), \boldsymbol{u}(t)) \leq 0 \qquad t \in [t_0, t_f]$$

$$\boldsymbol{g}(t_0, t_F, \boldsymbol{x}(t_0), \boldsymbol{x}(t_F), \boldsymbol{u}(t_0), \boldsymbol{u}(t_F)) \leq 0$$

Since the problem presented in Equation 9 is continuous and generally highly non-linear, it has no analytical solution. Therefore, discrete time histories of the states and controls are approximated using transcription. In DC, the time horizon is discretized into a number of time

Variable	Initial Condition	Lower bound	Upper bound	Final Condition
x, y [m]	Dep. Airport			Des. Airport
Altitude [m]		9000	**Ceiling**	
Mach [-]		**Min Mach**	**Max Mach**	
Mass (kg)	**80% MTOW**			**>OEW**
Thrust [kN]		**Max Thrust**	**Min Thrust**	
Flight path angle [deg]	0	0	0	0

Table II: *Table with constraints of the optimization problem. The bold variables are automatically imported from OpenAP as they are aircraft dependent. The origin and destination airports can be set manually by the user.*

intervals. In each of these intervals, a polynomial is fitted through the state and control variables. This polynomial is collocated with the system dynamics at the so-called collocation points, formulating a constraint to enforce the system behaviour. The approximating functions are implicit, as the solution is dependent on itself or that of the next time step [27]. The relationship between the amount of points at which discrete state information is available and the order of the approximating polynomial is notable; A polynomial of degree d requires at least $d+1$ pieces of information. Since the (implicit) information available at the nodes consists of the state value itself and its derivative, there are two pieces of information available per node. If the polynomial has a degree of four or higher, additional nodes are therefore required within each time interval, next to the nodes at the boundaries. The working principle of collocation is depicted in Figure 2. In this figure, the black dots represent the nodes at the start and end of the control interval. Between these nodes, the polynomial approximating the states is fitted. In this case, three collocation points are present. At these locations, the differences Δ between the state and control estimates for the polynomial and the actual system dynamics $f(\boldsymbol{x_c}, \boldsymbol{u_c})$ are obtained. These differences are forced to zero by imposing a constraint at each collocation point. As these constraints are enforced on each node, the result is a sparse matrix describing the relation between the node x_n and its neighbours x_{n-1} and x_{n+1}. This is the input to the non-linear programming solver.

For the translation of the optimal control problem to a non-linear programming problem, the symbolic framework of CasADi [28] is used. This tool provides a smooth interface to the non-linear programming solver IPOPT [29]. CasADi is highly flexible and allows users to set up their own transcription method. In this model, a fifth-degree polynomial is fitted through 3 collocation points per interval. A total of 30 control intervals is selected. The model is set up iteratively, meaning that upon failure with these initial settings, a new attempt is made with a different combination of collocation points and control intervals.

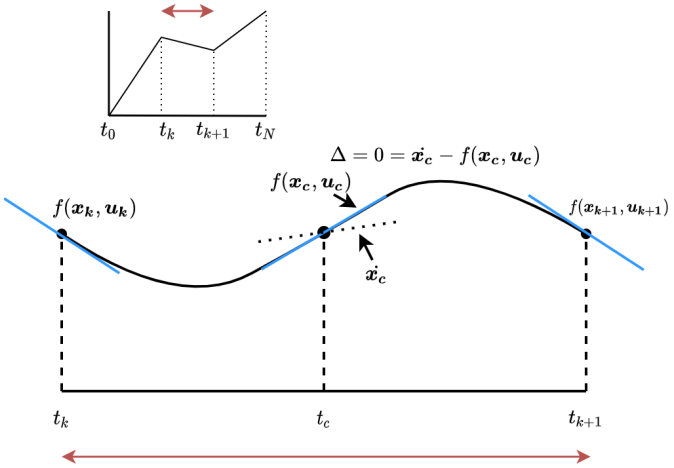

Figure 2: *General working principle of direct collocation. The time horizon is discretized into N control intervals. Three collocation points are located on each control interval. At these points, the dynamic constraint is enforced by collocating the estimated polynomial $\dot{\boldsymbol{x}}_c$ with the real system dynamics $f(\boldsymbol{x_c}, \boldsymbol{u_c})$.*

B. Genetic Algorithm

A possible way of optimizing a trajectory is by discretizing the solution space into a number of waypoints and evaluating all possible trajectories. However, as the number of possible trajectories scales exponentially with the amount of possible values per state and the number of waypoints, the problem quickly becomes too large to solve.

The concept behind GAs is to use the theory of evolution to converge to the global optimum, without evaluating all possible trajectories. Similarly to the Darwin's evolution theory, the fittest individuals of a species are able to pass down their set of genes to the next generation through the crossover step. By invoking random mutations to these genes, the global optimum will theoretically always be obtained without having to evaluate all possible scenarios. The developed algorithm defines a trajectory as an individual, which comprises a set of genes. Each gene is a waypoint containing information about the position and velocity at that specific location.

The core model consists of four phases, which are part of an iterative loop. They are presented in Figure 3. The first generation is created such that the generated trajectories are spread out over the possible solution space. The fitness evaluation then estimates the cost of each trajectory, in accordance with the optimization criteria. In the selection phase, routes in the generation are selected for later crossover. This model applies a fitness proportionate selection, otherwise known as the roulette wheel selection.

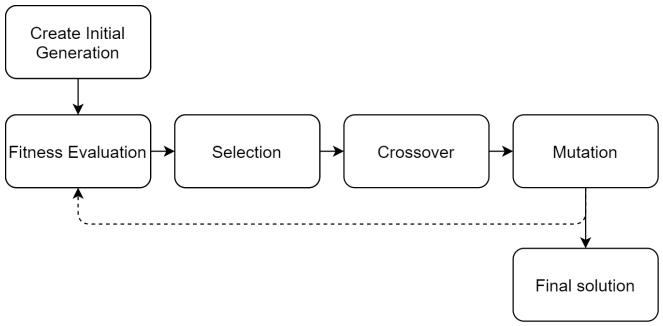

Figure 3: *Main phases of any genetic algorithm. An iterative heuristic search is applied, of which the results of each iteration are compared against some stopping criteria. If the criteria are met, the optimal solution is found.*

In such operator, the fitness of the trajectory determines the probability of selection according to Equation 10 [30], in which f_i is the fitness of trajectory i and $\boldsymbol{f}$ is the array holding all fitness values of the generation.

$$p_i = \frac{f_i - min(\boldsymbol{f})}{max(\boldsymbol{f}) - min(\boldsymbol{f})} \tag{10}$$

The crossover phase uses the genes of the selected individuals to create a new generation. Uniform crossover is applied, which considers each gene of the child individually when placing information from either parent A or parent B. The parents create two children with a set of contrasting genes.

An important parameter in this phase is the crossover rate, which determines how many parents are able to exchange their genes. A low crossover rate means that there will be more children cloned from one parent, while a higher crossover rate will increase the amount of children being created by the crossover process mentioned above.

The last phase of the iterative loop is the mutation of the newly created generation. A set of random genes is selected and randomly mutated. This random search is important to avoid getting stuck in local optima. The mutation rate dictates how many genes will be mutated.

In the genetic algorithm, the method developed by Hassanat et al. (2019) [31] is used. The researchers propose to dynamically decrease the mutation rate while increasing the crossover rate. The GA starts with a random search, which allows the algorithm to search for some global optima. Gradually, the search becomes more greedy until there are almost no mutations anymore. Hassanat found that this method works specifically well for a larger population size, which is the reason why the population size of TOEP-GA is 100. The list below presents the reader with an overview of the differences with generic genetic algorithms:

- Initially high mutation rate.
- Initially low crossover rate.
- Decrease mutation rate every generation.
- Increase crossover rate every generation.

IV. Benchmark Studies

The initial validity of both models is proven by presenting them with simple problems to which the solution is known. These preliminary results can be found in appendix subsection C. Thereafter, TOEP-GA is solely used as a means of verification for TOEP-DC because of its lower solution quality. This order of verification is selected to guarantee robustness of the final model.

The DC model is tested against the GA model by comparing the results for different objectives and airport combinations. For 50 flights, the trajectories are optimized for two different objectives: environmental cost and operating cost. TOEP-GA operates with 400 generations of 100 individuals each and an automatic stop when there has not been an improvement for 150 generations. TOEP-DC is set up with 30 control intervals, with each three collocation points.

The results of the analysis can be found in Figure 4a. In this figure, the relative difference between the two models is presented for each of the different performance indicators. Most of the discrepancies remain within two percent. They can be explained by the simplifications made in the GA. The coarseness of the grid on which the possible waypoints are located generally makes the resulting trajectory less optimal compared to the DC model. This can be seen in the figure, where the operating cost and climate cost are slightly lower for the DC and thus more optimal.

An example of one of the trajectories optimized in the benchmark studies is between London Heathrow airport and Los Angeles airport. The horizontal trajectory of the two models for this city pair can be found in Figure 4b. Here, the arrows represent the wind vector at 10,400 meters, which is the flight altitude of both the GA and the DC. Note that the two models produce nearly identical flight paths, with the DC model being more smooth than the GA model. The optimal trajectory found by the GA has an environmental cost of 72,600 USD, while the DC model finds one with an environmental cost of 71,400 USD[1]. This difference of 1.7% is in line with the average discrepancy in environmental cost between the two models. The average computational time of the direct collocation model is 17 seconds, which is 90% faster than the 165 seconds used by the genetic algorithm. The difference in computational efficiency could partly be explained by the fact that the interior point optimizer used in CasADi uses compiled C-code, which can greatly improve the computation speed. Besides, a genetic algorithm requires a larger amount of calculations to find the optimal solution.

V. Results

To grasp the impact of the optimized trajectories, it is imperative to compare the developed model with actual aircraft trajectories. Besides, the influence of optimizing

[1]Note that these numbers are provided to give the reader a feeling for the order of magnitude of the cost on a flight. The unit emission cost is associated with large uncertainty.

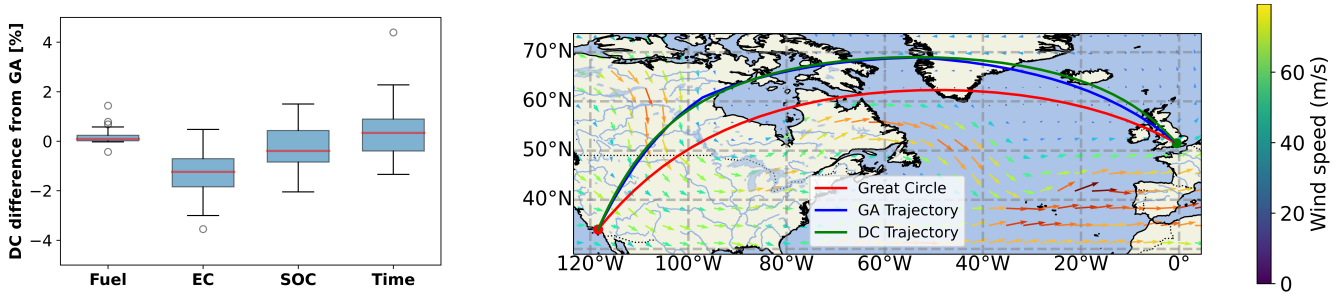

(a) *Difference between TOEP-GA and TOEP-DC obtained using 50 optimizations between different airports.*

(b) *Example optimization result of TOEP-GA and TOEP-DC between Heathrow airport and Los Angeles airport. Note that the result from the DC model is smooth, while the trajectory following from the GA is a combination of pre-defined grid points.*

Figure 4

for environmental purposes on the overall cost can be visualized by considering Pareto fronts. In these analyses of the TOEP approach, the TOEP-DC model is used to perform the optimization.

A. Actual flights vs. Optimal flights

Real flight trajectories on the first of December 2018 are obtained from the Eurocontrol R&D data archive [32]. Applicable flights for analysis are found using a filtration process; Only flights with a minimum flight time of one hour and a cruise altitude of at least 10 kilometres are selected. Besides, airports and aircraft which are not in the database of OpenAP are removed from the dataset. After filtration, the 50 routes with the highest flight frequency are selected. This leads to the selection of 130 flights for evaluation [2]. For more specific information about their characteristics, the reader is referred to subsection D. For each trajectory, the performance indicators flight time, EC, SOC and fuel usage are obtained using the flight data points, which are between 5 and 10 minutes apart. To accurately evaluate the theoretical optimal trajectories for each of the selected flights, the optimization is performed between the first and last logged latitude-longitude combinations above 10 kilometres altitude. All flights are optimized for both environmental cost and operating cost.

In Figure 5, the average differences between the actual and optimal trajectories are displayed. The x-axis specifies the type of optimization. On average, the environmental cost can be reduced with 6.6%. Note that the operating cost also decreases in this scenario, with 2.5%. This is due to the partly aligned operating and environmental cost functions. Both are driven down by a reduction in fuel usage, which is 4.6% in this scenario. If the flight path angle is not constrained at 0, the optimal trajectory would have a continuously increasing altitude. Such a cruise climb would further reduce the environmental cost with 0.4%.

[2]The justification for the selection of this amount of flights is the computational time associated with the evaluation of a trajectory.

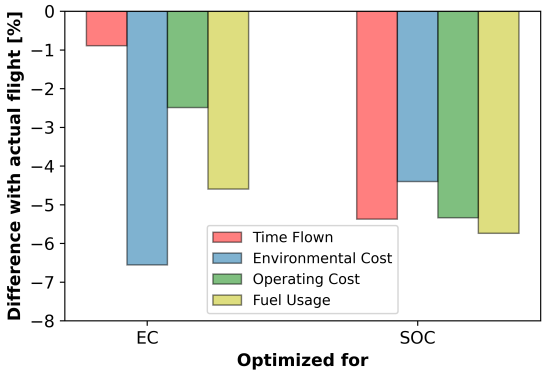

Figure 5: *Comparison between results of 130 actual flights and those of optimized flights. Two types of optimization are performed.*

On the right-hand side of the plot, a comparison with the SOC optimal scenario is provided. Note that the flight time and fuel usage have been reduced significantly more compared to the other scenario. As the operating cost function (Equation 7) has a linear relationship with time and fuel, the resulting decrease in operating cost is expected. The operating cost is mostly driven by fuel usage, which results in a further reduction of fuel used compared to the EC-optimal scenario. This contributes to the large reduction in environmental cost on the right-hand side of the figure and at the same time explains why the environmental cost is reduced more in SOC-optimality compared to operating cost in EC-optimality.

Airlines also optimize for a cost function when determining their routing strategy, which is similar to the simplified operating cost function adopted in this study. Therefore, one would expect the performance indicators in SOC-optimality to be similar to those of the actual trajectories. The cause of their dissimilarity is the underlying assumption of direct routing in TOEP. Whereas airlines often fly specific routes to avoid airspace or to follow constraints imposed by air traffic control, the algorithm does not consider any of these constraints.

This provides insights on the overall potential of climate-optimal routing. These results confirm that efforts should be made to loosen airspace constraints and work towards the implementation of direct routing strategies. An example of a real trajectory with inefficient routing can be found in appendix subsection E.

B. Operating cost vs. environmental cost optimality

Whereas the previous analysis provided useful insights on the effectiveness of TOFEI, it is interesting to consider a situation in which the efficiency gained by direct routing is factored out. Minimum operating cost is a suitable reference, as airlines often optimize for this or a similar objective function to determine which route to fly. To understand the effect of flight duration on these results, three types of flights are established. A flight shorter than 3 hours is considered short haul, a medium haul flight is between 3 and 6 hours, and flights longer than 6 hours are long haul.

Table III presents the environmentally-optimal results compared to the SOC-optimal scenario. Note that overall, the environmental cost reduction is 2.0%. As expected, this is significantly smaller compared to the value obtained in Figure 5.

For short flights, the environmental cost can only be reduced with 1.2% while the operating cost increases with 3.1%. These types of flight have a small optimization potential, as there are little wind variations and the relative search space is small because of the limited length of the flight. As a result, the difference between the two scenarios is mainly in altitude and velocity. Hence, only a small reduction in environmental cost is observed.

For long flights, the environmental cost can be decreased with 2.7%. This is the result of more wind variations and a larger relative search space, leading to a higher optimization potential. This will naturally yield a larger difference in environmental cost compared to short haul flights. At the same time, the associated operating cost does not follow this trend. This seems to be the result of the relative flight time reduction between long haul and short haul flights. However, the optimal combination between altitude, true airspeed and fuel usage to obtain minimal environmental impact is nonlinear. Therefore, additional investigations are required to adequately determine which of these variables drive the environmental cost most and how this impacts the difference in operating cost.

C. Pareto Optimality

Multiple Pareto fronts are obtained using the mix function (Equation 8) and a range of cost indices between 0 and 1. The weight parameters l_{soc} and l_{ec} are changed linearly changed to obtain a Pareto front. The plots are generated assuming an Airbus A388 aircraft model. The origin and destination cities are London and Los Angeles, respectively.

Figure 6a displays the resulting Pareto fronts. One might note an increase in horizontal spread of the lines as the cost index increases. This implies that a higher CI yields more expensive environmental impact when optimizing for operating cost. This is a natural result of the operating cost function. With an increasingly dominated weight of time cost, it becomes more important to optimize this parameter than fuel cost. The flight time can only be reduced by flying faster and more direct, which is conflicting with the environmental cost. The result is the increasing ranges of environmental cost.

The figure clearly visualizes a linear relationship between the operating cost and the cost index. Increasing the cost index will yield a lower operating cost. A high cost index implies that the time cost becomes dominant in the operating cost function, while at a low cost index the fuel cost will dominate. As the unit cost of time is higher than that of fuel, this might seem counter-intuitive at first. However, the amount of fuel used in a flight is generally significantly higher compared to the flight time. For this specific flight, the average fuel flow is 3.37 kg/s, which explains the linear decrease in SOC as the cost index is increased.

As this behaviour is the especially prominent in the figure, the Pareto front for a cost index of 0.5 is isolated in Figure 6b to observe the relation between operating cost and environmental impact in more detail. The contour of this plot is exactly the same as for other CI values. For this cost index, the environmental cost can fluctuate with 2.9% between the two most extreme optimization scenarios. At the same time, the operating cost fluctuates with 2.0%. This is in the same order of magnitude as the values found in Table III for long haul flights.

D. Sensitivity Studies

The unit emission cost for each species is paired with a relatively high uncertainty. It is imperative to investigate their effects on the model. To this end, a sensitivity study is performed. First, the unit cost is sampled from one of the distributions presented in appendix subsection B while keeping other cost parameters constant at their mean value. This Monte Carlo simulation yields a distribution of environmental cost that provides insights into both the effect of the uncertainty and the importance of the accuracy of the unit emission cost per species.

Besides sampling individual species, the sensitivity study incorporates an analysis of the overall range of possible environmental cost values by sampling from all individual unit cost distributions at the same time. In this sensitivity study, 1000 samples are taken to find the optimal trajectory between London Heathrow airport and Los Angeles airport with the arbitrarily chosen A380 aircraft.

The results of the sensitivity study are given in Figure 7. Here, the blue lines indicate the resulting distribution from individual sampling. In red, the results are given for when all species are sampled at the same time. The mean of

Flight type	# Flights	Flight distance [%]	Flight time [%]	Fuel usage [%]	EC [%]	SOC [%]
Overall	130	+0.7	+4.4	+1.2	-2.0	+2.8
Short haul	50	+1.4	+4.6	+1.1	-1.2	+3.1
Medium haul	44	+0.7	+4.3	+1.3	-2.2	+2.8
Long haul	36	-0.5	+4.2	+1.2	-2.7	+2.4

Table III: *Comparison between results for SOC optimality and EC optimality, split by duration.*

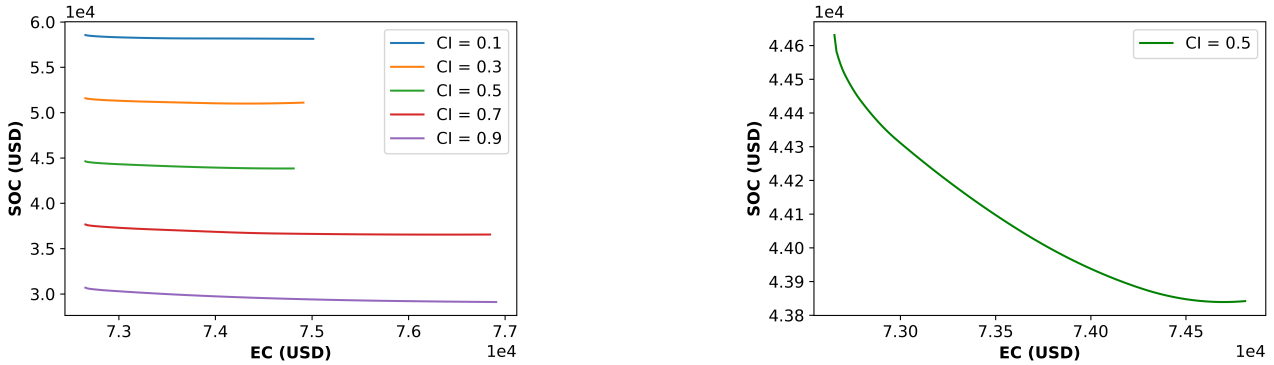

(a) *Pareto fronts for different cost indices (CI) in a case study between London Heathrow airport and Los Angeles airport.*

(b) *Pareto front for a cost index (CI) of 0.5 in a case study between London Heathrow airport Los Angeles airport.*

Figure 6

this distribution is depicted by the dashed green line, at 73,200 USD. The green solid lines correspond to the 90% confidence interval of the combined sampling scenario, which is located between 15,000 and 170,000 USD. It is evident that the impact of the uncertainty in both NO_x and CO_2 is multiple orders of magnitude larger than that of H_2O, HC and CO. This has two causes. First, the majority of the environmental cost consists of CO_2 and NO_x, with an average share of 23% and 76%, respectively. Moreover, the uncertainty of NO_x is multiple orders of magnitude greater than that of the other species, as found in Table I.

When sampling from all distributions at the same time, the mean environmental cost is similar to the 72,800 USD one obtains when using the mean unit cost values as input, which helps prove the validity of the obtained distribution. The right tail of the data distribution is longer than the left tail, which is the result of the unit cost distributions each having a similar shape. Note that the environmental cost values encountered in the sensitivity analysis of H_2O, HC and CO are larger than the mean cost found in the combined study. This is caused by the fact that in this scenario, the NO_x and CO_2 values are kept constant at their mean value, which is above their mode. The right skewed nature of their species distributions causes the observed phenomenon.

E. Discussion

The results presented in this study show that optimal routing strategies can significantly contribute to the mitigation of aviation climate effects. When optimizing solely for climate impact, the average environmental cost could be reduced with 6.6% compared to current operations.

When conscious of the difference in scope and model set-up of other research, one can perform a comparison between this study and others. Research by Tian et al. (2019) [17] also considered a monetary environmental cost. In their first paper, the researchers found that optimizing for this metric yields a reduction of 3.3% compared to optimality for operating cost. This is similar to the values found in this study. One major difference between the two studies is that Tian performed a 2D search, whereas TOEP incorporates a 3D search for optima.

Yamashita et al. (2020) [10] found that when compared to cost-optimal trajectories, the average temperature response could be reduced with up to 68%. This is a significant difference with the results presented in this paper. Two reasons for this major dissimilarity are found in the scope of the studies. First, the temperature response obtained by Yamashita is measured in Kelvin $\cdot 10^{-7}$. As the absolute change in temperature is small between objectives, Yamashita naturally finds a larger change when compared to the EC as a cost metric. Besides, Yamashita considered the formation of contrails. The impact of these aviation-induced clouds on the results obtained by the researchers is found to be significant.

Some limitations can be identified in the scope of the research presented in this paper. First, environmental-optimality is achieved by optimizing an objective function which does not take into consideration contrails. In a recent study, Lee et al. [33] find that contrails formed due to condensed exhaust gas contribute for up to 50% to aviation-induced global warming. Due to the large uncertainty associated with contrail cost, they have been left out of the scope of this study. As more research is done

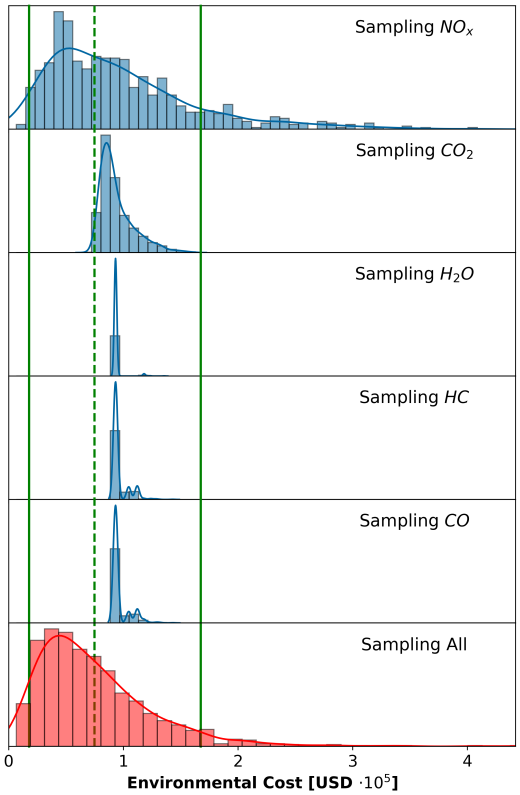

Figure 7: *Sensitivity analysis results. In blue, the distribution obtained by sampling one species are presented while the red distribution represents results from sampling all unit cost values at the same time. The green dotted line represents the mean value of the red distribution.*

in this field, one can expect more accurate modelling to enable the inclusion of their effects in future work. Besides, this study only considered the cruise phase of flight. It would be interesting for future research to investigate the options of incorporating a multiphase optimization problem into TOEP-DC, to enable optimization of the full flight. Another limitation imposed by the scope of this research is the initial mass assumption. This study assumes the initial mass as a constant fraction of the maximum take-off weight. Upon comparison with actual flights this raises the question as to how much this constraint influences the results. As the Eurocontrol dataset does not provide the mass of the aircraft, the constraint is kept. A more thorough analysis should be performed to assess the impact the starting mass has on the results.

The main limitations of the optimization criteria used in this study are threefold. First, specific airspace constraints have not been considered. This resulted in a more optimal environmental cost compared to real flights, even when optimizing for operating cost. Whereas this is an unintended side effect of the model, it does show the significant possibilities of direct routing. Furthermore, the path angle of aircraft is zero throughout the trajectory. This meant that TOEP selected the best constant altitude to fly at. An investigation shows that if this constraint is not present, the environmental cost could decrease with an additional 0.4%. For future studies, it is recommended to set up an optimization in which the flight path angle is allowed to vary for a limited time. Finally, large uncertainties are introduced by using the emission cost values from Grobler et al. (2019) [23]. It is imperative that the quality of the solution produced by TOEP is directly correlated with the certainty associated with the unit cost of emission per species. The sensitivity study in this paper provides the range of possible environmental cost values due to this uncertainty. The unit cost values, especially that of NO_x, should be more certain before the environmental cost function can be used as an objective in real life optimization. Therefore, it is worth investigating a non-monetary objective function. The global warming potential values presented in the research by Förster et al. (2016) could provide an adequate starting point [15].

VI. Conclusions

The aim of this paper was to present an open approach which takes the next step in Trajectory Optimization For Environmental Impact (TOFEI) research by incorporating a more realistic scope compared to the status quo: considering wind, variable Mach number and a comprehensive environmental impact metric. This study developed the Trajectory Optimizer for Environmental Purposes (TOEP), which is based on the open aircraft performance model OpenAP and the non-linear optimizer CasADi.

Two models were established to find optimal trajectories. A genetic algorithm was established to verify the results of the direct collocation model. To model the environmental impact, a monetary environmental cost metric was used. Upon comparison between the two approaches, some minor discrepancies were found. These could be attributed to the set-up of the genetic algorithm, specifically the coarseness of its grid. In future studies, the developed genetic algorithm could remain relevant. As the computational efficiency of the direct collocation model is influenced by the initial guess that is provided, the genetic algorithm could perform an initial search to find an adequate starting point.

In a comparison with real-life flights, TOEP performed specifically well in optimizing for the environmental cost. Compared to a set of 130 actual flights, a reduction of 6.6% in environmental impact can be achieved. The analysis confirmed the consensus that reducing the number of airspace constraints helps reduce the environmental impact of aviation. Moreover, a comparison was performed between optimization results for two different objective functions. The environmental cost is 2.0% lower when optimizing for this parameter compared to the environmental cost when optimizing for operating cost. Specifically, long flights are

found to be suitable for optimization.

A sensitivity study reveals that the uncertainty in unit emission cost of NO_x has the most profound impact on the environmental cost. The large uncertainty in this species leads to large fluctuations in the outcome. For an arbitrary long haul flight between Los Angeles airport and London Heathrow airport with an airbus A380 aircraft, one can be 90% certain that the environmental cost is between 15,000 and 170,000 USD. More research towards the unit environmental cost should be performed, specifically focusing on that of NO_x and contrails.

This study has demonstrated the process of trajectory optimization for environmental impact based on new environmental cost metrics of flights. A realistic test case is applied to manifest the future step towards implementation. Most importantly, built upon open models and tools, TOEP gives stakeholders the opportunity to discover trajectory optimization for environmental purposes in an open framework.

References

[1] Eurocontrol. 'EUROCONTROL Five-Year Forecast 2020-2024 European Flight Movements and Service Units'. In: November (2020).

[2] Ahmad Baroutaji et al. 'ICAO 2019 Environment Report'. In: *2019 Aviation and the Environment Report* 43.February (2019), pp. 21–22.

[3] Steve H.L. Yim et al. 'Global, regional and local health impacts of civil aviation emissions'. In: *Environmental Research Letters* 10.3 (2015). DOI: 10.1088/1748-9326/10/3/034001.

[4] Piers Forster et al. 'Changes in atmospheric constituents and in radiative forcing. Chapter 2'. In: *Climate Change 2007. The Physical Science Basis*. United Kingdon: Cambridge University Press, 2007.

[5] J.S. Fuglestvedt et al. 'Transport impacts on atmosphere and climate: Metrics'. In: *Atmospheric Environment* 44.37 (2010). Transport Impacts on Atmosphere and Climate: The ATTICA Assessment Report, pp. 4648–4677. DOI: https://doi.org/10.1016/j.atmosenv.2009.04.044.

[6] Nicolas E. Antoine and Ilan M. Kroo. 'Framework for Aircraft Conceptual Design and Environmental Performance Studies'. In: *AIAA Journal* 43.10 (2005), pp. 2100–2109. DOI: 10.2514/1.13017.

[7] Hooi Ling Khoo and Lay Eng Teoh. 'A bi-objective dynamic programming approach for airline green fleet planning'. In: *Transportation Research Part D: Transport and Environment* 33 (2014), pp. 166–185. DOI: https://doi.org/10.1016/j.trd.2014.06.003.

[8] Eurocontrol. *European ATM Network Fuel Inefficiency Study*. Tech. rep. 2020.

[9] Javier García-Heras, Manuel Soler and Francisco J. Sáez. 'Collocation methods to minimum-fuel trajectory problems with required time of arrival in ATM'. In: *Journal of Aerospace Information Systems* 13.7 (2016), pp. 243–265. DOI: 10.2514/1.I010401.

[10] Hiroshi Yamashita et al. 'Newly developed aircraft routing options for air traffic simulation in the chemistry–climate model EMAC 2.53: AirTraf 2.0'. In: *Geoscientific Model Development* 13.10 (2020), pp. 4869–4890. DOI: 10.5194/gmd-13-4869-2020.

[11] Hugo Pervier et al. 'Application of Genetic Algorithm for Preliminary Trajectory Optimization'. In: *SAE International Journal of Aerospace* 4.2 (2011), pp. 973–987. DOI: 10.4271/2011-01-2594.

[12] Hendrikus G. Visser and Sander Hartjes. 'Economic and environmental optimization of flight trajectories connecting a city-pair'. In: *Proceedings of the Institution of Mechanical Engineers, Part G: Journal of Aerospace Engineering* 228.6 (2014), pp. 980–993. DOI: 10.1177/0954410013485348.

[13] V. Grewe et al. 'Aircraft routing with minimal climate impact: the REACT4C climate cost function modelling approach (V1.0)'. In: *Geoscientific Model Development* 7.1 (2014), pp. 175–201. DOI: 10.5194/gmd-7-175-2014.

[14] Marianne Jacobsen and Ulf T. Ringertz. 'Airspace constraints in aircraft emission trajectory optimization'. In: *Journal of Aircraft* 47.4 (2010), pp. 1256–1265. DOI: 10.2514/1.47109.

[15] Stanley Förster et al. 'A toolchain for optimizing trajectories under real weather conditions and realistic flight performance'. In: October (2016).

[16] Cesar Celis et al. 'Theoretical optimal trajectories for reducing the environmental impact of commercial aircraft operations'. In: *Journal of Aerospace Technology and Management* 6.1 (2014), pp. 29–42. DOI: 10.5028/jatm.v6i1.288.

[17] Yong Tian et al. 'Cruise flight performance optimization for minimizing green direct operating cost'. In: *Sustainability (Switzerland)* 11.14 (2019). DOI: 10.3390/su11143899.

[18] Yong Tian et al. '4D Trajectory Optimization of Commercial Flight for Green Civil Aviation'. In: *IEEE Access* 8 (2020), pp. 62815–62829. DOI: 10.1109/ACCESS.2020.2984488.

[19] Hans Hersbach et al. 'Operational global reanalysis: progress, future directions and synergies with NWP'. In: 12 (2018). DOI: 10.21957/tkic6g3wm.

[20] Junzi Sun, Jacco M. Hoekstra and Joost Ellerbroek. 'OpenAP: An open-source aircraft performance model for air transportation studies and simulations'. In: *Aerospace* (2020). DOI: 10.3390/AEROSPACE7080104.

[21] Roberto Salvador Félix Patrón and Ruxandra Mihaela Botez. 'Flight trajectory optimization through genetic algorithms for lateral and vertical integrated navigation'. In: *Journal of Aerospace Information Systems* 12.8 (2015), pp. 533–544. DOI: 10.2514/1.I010348.

[22] E. Gallo et al. 'Advanced Aircraft Performance Modeling for ATM: BADA 4.0 Results'. In: *2006 ieee/aiaa 25TH Digital Avionics Systems Conference*. 2006, pp. 1–12. DOI: 10.1109/DASC.2006.313660.

[23] Carla Grobler et al. 'Marginal climate and air quality costs of aviation emissions'. In: *Environmental Research Letters* 14.11 (2019). DOI: 10.1088/1748-9326/ab4942.

[24] Donald E Hilt and Donald W Seegrist. *Ridge, a computer program for calculating ridge regression estimates*. Vol. 236. Department of Agriculture, Forest Service, Northeastern Forest Experiment ..., 1977.

[25] M. A. Burris. 'Cost index estimation'. In: *IATA 3rd Airline Cost Conference* (Aug. 2015), pp. 1–27.

[26] Matthew Kelly. 'An introduction to trajectory optimization: How to do your own direct collocation'. In: *SIAM Review* 59.4 (2017), pp. 849–904. DOI: 10.1137/16M1062569.

[27] F. Topputo and C. Zhang. 'Survey of direct transcription for low-thrust space trajectory optimization with applications'. In: *Abstract and Applied Analysis* 2014 (2014). DOI: 10.1155/2014/851720.

[28] Joel A.E. Andersson et al. 'CasADi: a software framework for nonlinear optimization and optimal control'. In: *Mathematical Programming Computation* 11.1 (2019), pp. 1–36. DOI: 10.1007/s12532-018-0139-4.

[29] Andreas Wächter and Lorenz T Biegler. 'On the implementation of an interior-point filter line-search algorithm for large-scale nonlinear programming'. In: *Mathematical programming* 106.1 (2006), pp. 25–57.

[30] Tobias Blickle and Lothar Thiele. 'A Comparison of Selection Schemes Used in Evolutionary Algorithms'. In: *Evolutionary Computation* 4.4 (Dec. 1996), pp. 361–394. DOI: 10.1162/evco.1996.4.4.361. eprint: https://direct.mit.edu/evco/article-pdf/4/4/361/1492921/evco.1996.4.4.361.pdf.

[31] Ahmad Hassanat et al. 'Choosing Mutation and Crossover Ratios for Genetic Algorithms — A Review with a New Dynamic Approach'. In: *Information* (2019). DOI: 10.3390/info10120390.

[32] EUROCONTROL. *R&D data archive*. https://www.eurocontrol.int/dashboard/rnd-data-archive. 2015.

[33] D S Lee et al. 'The contribution of global aviation to anthropogenic climate forcing for 2000 to 2018'. In: *Atmospheric Environment* (2020), p. 117834. DOI: 10.1016/j.atmosenv.2020.117834.